

Supplement of Atmos. Chem. Phys., 14, 9013–9027, 2014
<http://www.atmos-chem-phys.net/14/9013/2014/>
doi:10.5194/acp-14-9013-2014-supplement
© Author(s) 2014. CC Attribution 3.0 License.



Supplement of

**One-year observations of size distribution characteristics of major aerosol constituents at a coastal receptor site in Hong Kong –
Part 1: Inorganic ions and oxalate**

Q. Bian et al.

Correspondence to: J. Z. Yu (jian.yu@ust.hk)

Table S1 Mass median aerodynamic diameter of distribution modes at UST (unit: μm)

	1996-1997 ¹		2008 ²		2011-2012 (this study)	
	Winter	Summer	Winter	Summer	Winter	Summer
SO_4^{2-}	0.20	0.27±1.30	0.27±1.30	0.25±1.34	0.26±1.25	
	0.58	0.80±1.46	0.95±1.53	0.83±1.54	0.84±1.50	
	4.20	3.34±2.27	4.17±2.07	5.13±2.06	5.03±2.16	
NH_4^+	0.21	0.26±1.36	0.24±1.37	0.26±1.35	0.26±1.26	
	0.56	0.78±1.54	0.94±1.69	0.82±1.53	0.84±1.50	
	5.70	2.14±1.50	4.69±2.07	5.02±2.35	5.06±2.17	
NO_3^-	0.14	0.15±1.39	0.24±1.40			
	0.46	0.78±1.75	0.85±1.46	0.77±2.18	0.88±1.44	
	3.95	3.37±1.50	2.50±1.52	3.40±1.49	2.96±1.53	
		7.16±1.41	6.94±1.51	7.19±1.42	6.83±1.44	
$\text{C}_2\text{O}_4^{2-}$		0.25±1.65	0.24±1.37	0.12±1.51	0.29±1.28	
		0.88±1.70	0.90±1.64	0.92±2.02	0.77±1.49	
		4.35±2.04	4.22±2.05	5.25±1.64	4.58±2.12	

¹Zhuang et al., 1999b;²Yu et al, 2010.**Table S2.** Comparisons of PMF-modeled and measured concentrations of species used in the PMF analysis of the coarse-mode species data.

	SO_4^{2-}	NO_3^-	NH_4^+	K^+	Na^+	Mg^{2+}	Cl^-	Ca^{2+}	$\text{PM}_{2.5} \text{Si}^1$
R^2	0.79	0.99	0.97	0.79	0.99	0.97	0.99	0.83	0.90
Slope	0.73	0.94	1.03	1.28	1.01	0.98	0.96	0.98	0.67
Intercept	0.19	0.15	-0.015	-0.039	0.014	0.005	0.068	-0.013	0.12

¹ $\text{PM}_{2.5} \text{Si}$ data are used as tracers for bulk dust particles, as coarse mode Si data is not available.

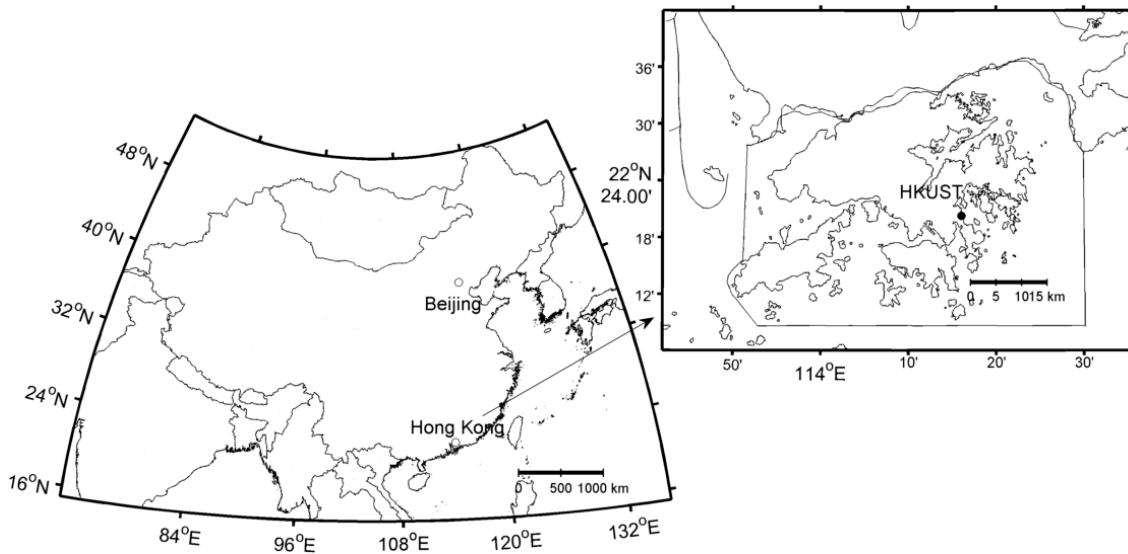


Figure S1. Sampling location in this study

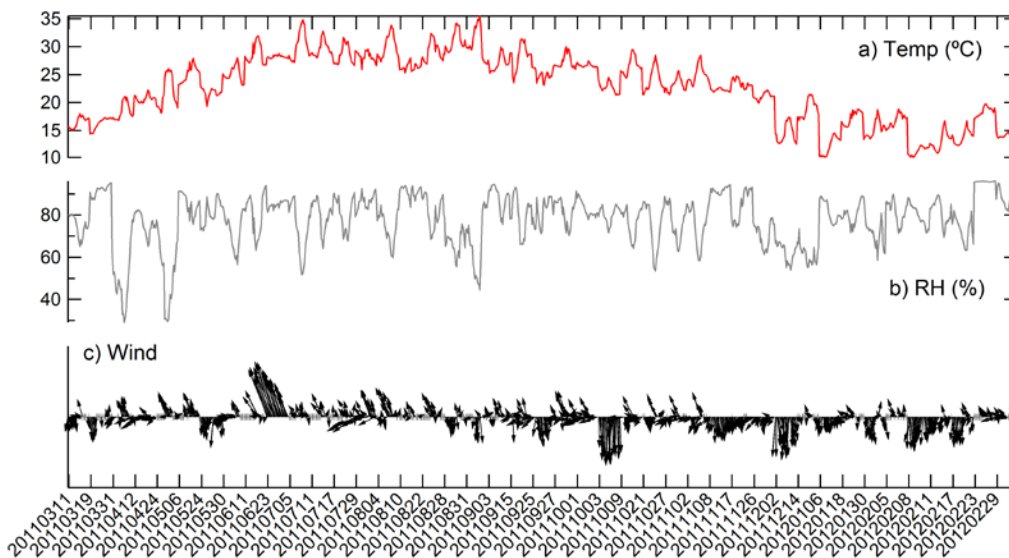


Figure S2 Hourly temperature (°C), RH (%) and wind vector during the sampling days.

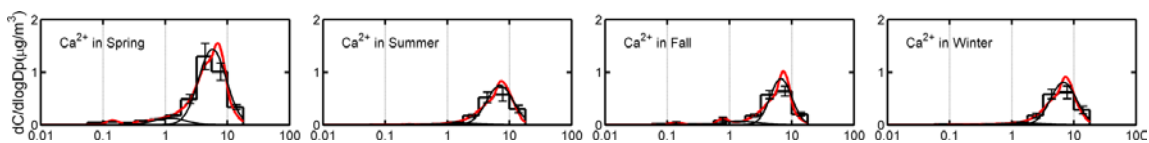


Figure S3 The Twomey algorithm results in skewed log-normal distribution curves of Ca^{2+} (red curves) when assuming one fine mode and one coarse mode. The measured data are shown as histograms.

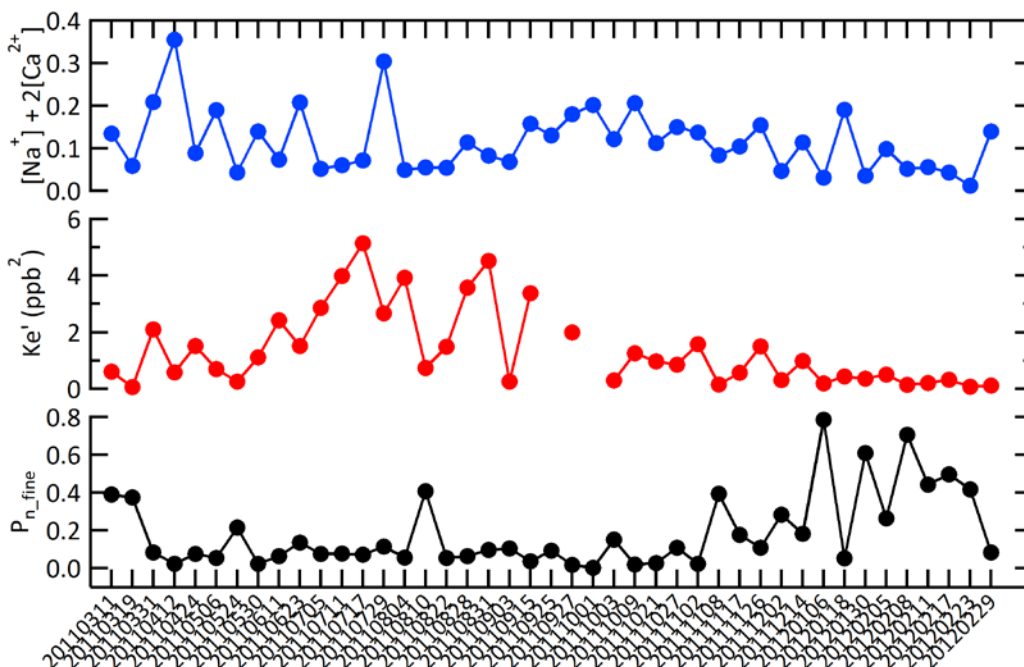


Figure S4 Time series of $[\text{Na}^+] + 2[\text{Ca}^{2+}]$ abundance in coarse particles ($3.2\text{--}18\ \mu\text{m}$), modified NH_4NO_3 dissociation equilibrium constant (K_e'), and percentage of nitrate in the fine mode (P_n) ($<1.8\ \mu\text{m}$). K_e' is dependent on temperature, relative humidity, and ion strength in aerosol liquid phase.

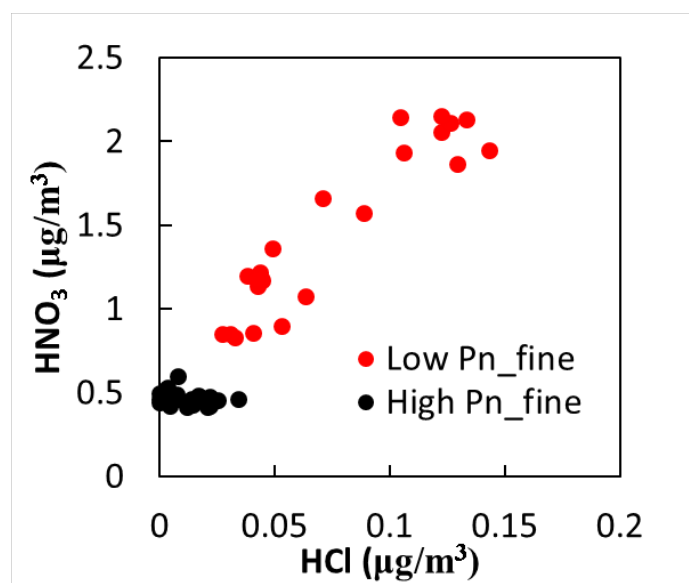


Figure S5 Correlations between gaseous HCl and HNO₃ in the hours during collection samples of low P_{n_fine} and high P_{n_fine} . P_{n_fine} is the percentage of nitrate in the fine mode (<30%).

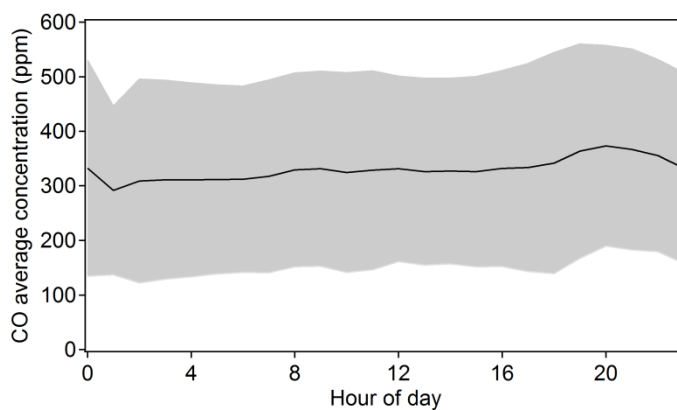


Figure S6 Diurnal variation of CO on the sampling days

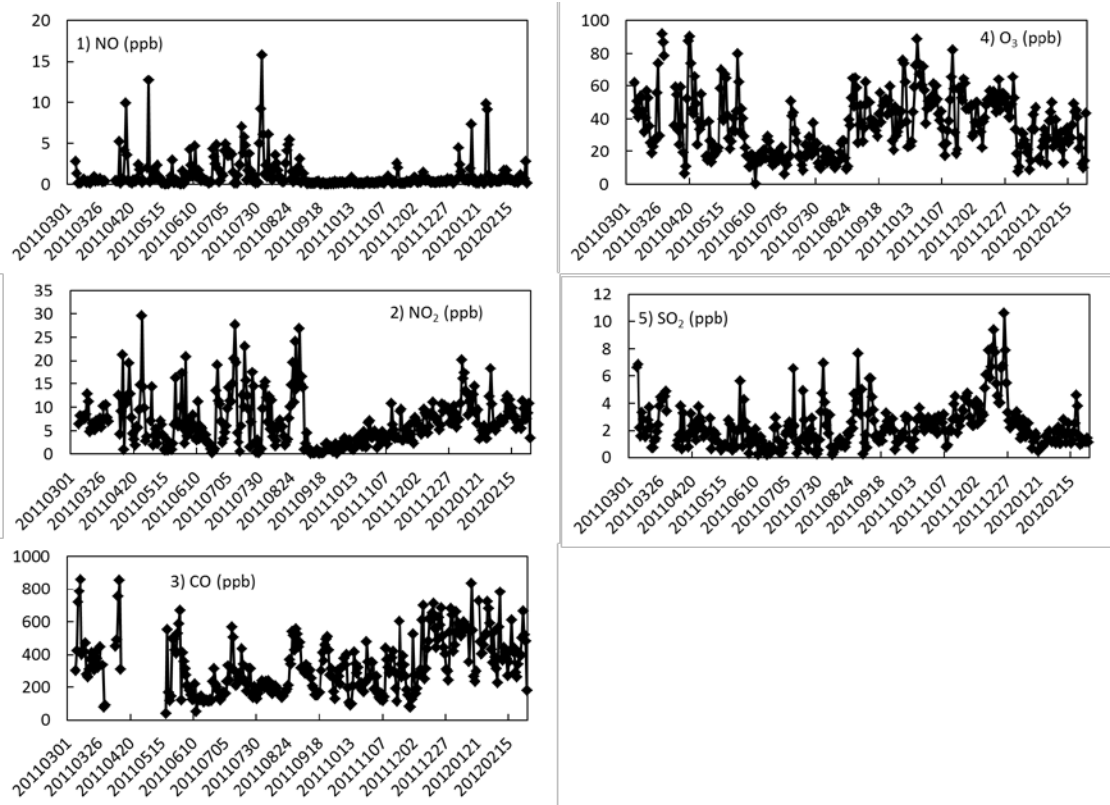


Figure S7. Time series of gas concentration level for gas species including NO, NO₂, CO, O₃, and SO₂ from March 2011 to February 2012. Date is in the format of YYYYMMDD.

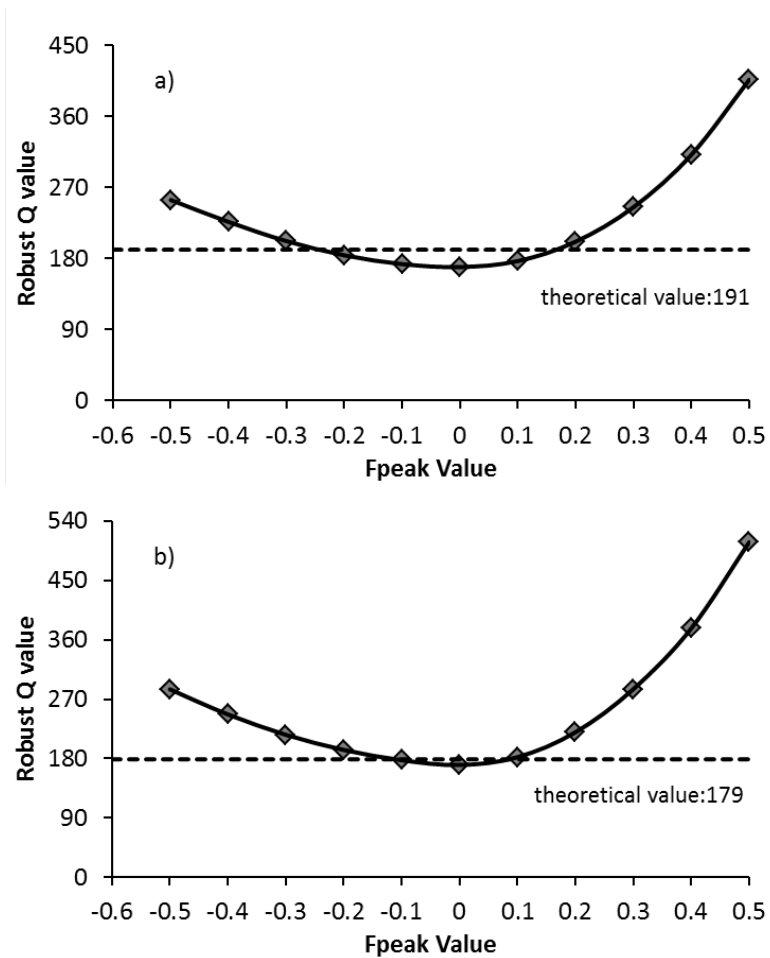


Figure S8. Robust Q as a function of Fpeak value from -0.5 to 0.5 in the PMF analysis of (a) the size-segregated sulfate data; (b) the coarse sulfate data. The dot line represents the theoretical value and is included to serve as a reference.

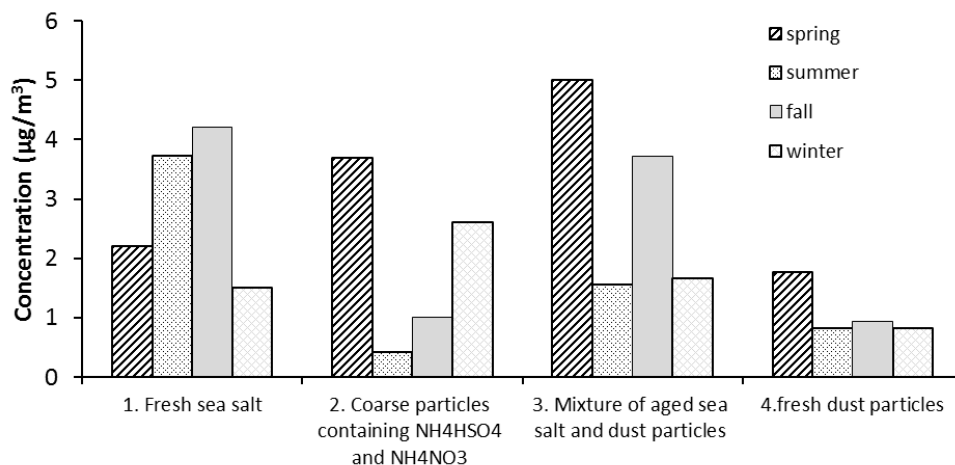


Figure S9. The seasonal variation in source contributions by the four PMF-derived sources

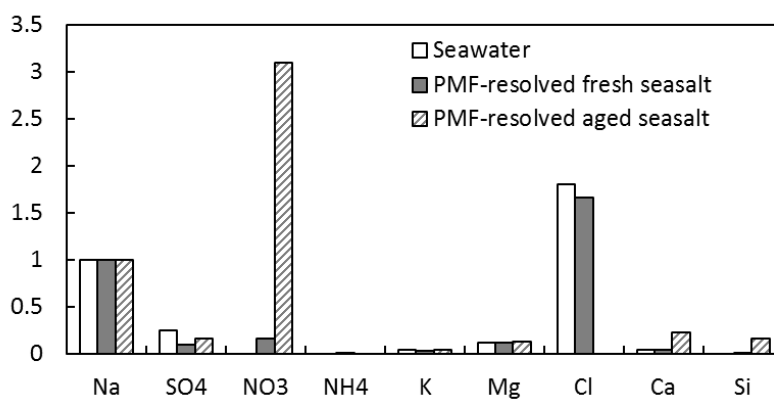


Figure S10. Comparison between seawater composition and PMF-derived factors of fresh sea salt and aged sea salt. All the species are normalized against Na⁺. The source profile of seawater with salinity of 35‰ is taken from Millero and Sohn (1992).